J. Mol. Biol. (1987) **193**, 571–578

LETTERS TO THE EDITOR

Nuclear Magnetic Resonance Study of the Solution Structure of α1-Purothionin

Sequential Resonance Assignment, Secondary Structure and Low Resolution Tertiary Structure

The solution structure of the 45-residue plant protein, α1-purothionin, is investigated by nuclear magnetic resonance (n.m.r.) spectroscopy. Using a combination of two-dimensional n.m.r. techniques to demonstrate through-bond and through-space (<5 Å) connectivities, the ^{1}H n.m.r. spectrum of α1-purothionin is assigned in a sequential manner. The secondary structure elements are then delineated on the basis of a qualitative interpretation of short-range nuclear Overhauser effects (NOE) involving the NH, CαH and CβH protons. There are two helices extending from residues 10 to 19 and 23 to 28, two short β-strands from residues 3 to 5 and 31 to 34 which form a mini anti-parallel β-sheet, and five turns. In addition, a number of long-range NOE connectivities are assigned and a low resolution tertiary structure is proposed.

The thionins and their homologues constitute a set of ubiquitous low molecular weight protein toxins (M_r ~5000) throughout the plant kingdom (Mak & Jones, 1976*a*,*b*; Jones *et al.*, 1982). These toxins are haemolytic, lyse a wide variety of mammalian cells and cause skin and skeletal muscle contraction (Anderson & Johannson, 1973; Okada & Vashizumi, 1973; Carrasco *et al.*, 1971). In addition, they can substitute for specific thioredoxins under favourable circumstances (Wada & Buchanan, 1981). At the present time, however, little is known about the structures of the thionins beyond their primary structure.

The amino acid sequences of the thionins display 40 to 50% homology with respect to crambin (Teeter *et al.*, 1981), a hydrophobic, water-insoluble plant protein with biological activity not yet known (Van Etten *et al.*, 1965), whose crystal structure has been solved to very high resolution by X-ray and neutron diffraction (Teeter & Hendrickson, 1979; Hendrickson & Teeter, 1981; Teeter & Kossiakoff, 1982). Moreover, crambin and the thionins have nearly identical lengths (46 and 45 residues, respectively) and the same pattern of disulphide linkages, with an additional one in the thionins. It has, therefore, been proposed that the three-dimensional structures of crambin and the thionins may also be similar (Teeter *et al.*, 1981; Whitlow & Teeter, 1985). Some evidence to support this hypothesis has come from c.d.† and laser Raman spectroscopy as well as from secondary structure prediction studies, which suggested that the secondary structures of crambin and the thionins are similar (Williams & Teeter, 1984; Whitlow & Teeter, 1985; Whitlow, 1986). Additionally, the general appearance of the n.m.r. spectra of five thionins were found to be similar, and one-dimensional NOE measurements irradiating the aromatic proton resonances of Tyr13 of two thionins, α1-purothionin and β-hordothionin, suggested that its spatial neighbours are similar to those of Phe13 in crambin (Lecomte *et al.*, 1982). On this basis three-dimensional models of one thionin, namely α1-purothionin, and the related protein viscotoxin A3 from mistletoe, were derived by appropriate substitution of the amino acid side-chains of crambin followed by energy minimization (Whitlow & Teeter, 1985). In the case of α1-purothionin crystals have also been obtained, but attempts to solve its structure by molecular replacement and Patterson search techniques using the predicted structure have so far been unsuccessful (Whitlow, 1986). This suggests that the difference in the structures of α1-purothionin and crambin may be more substantial than was supposed.

An alternative approach to X-ray crystallography that can be used to solve the three-dimensional structures of small proteins is n.m.r. spectroscopy (Wüthrich *et al.*, 1982; Williamson *et al.*, 1985; Kline *et al.*, 1986). This mainly involves the application of NOE measurements to obtain a large set of approximate interproton distances which can then be used as the basis of a three-dimensional structure determination using either distance geometry (Havel & Wüthrich, 1985; Braun & Go, 1985) or restrained molecular dynamics (Clore *et al.*, 1985, 1986*a*; Kaptein *et al.*, 1985;

† Abbreviations used: c.d., circular dichroism; n.m.r., nuclear magnetic resonance; NOE, Nuclear Overhauser effect; NOESY, two-dimensional NOE spectroscopy; DQF-COSY, double quantum filtered two-dimensional correlated spectroscopy; HOHAHA, two-dimensional homonuclear Hartmann–Hahn spectroscopy; D, ^{2}H.

0022-2836/87/030571-08 $03.00/0

Brünger *et al.*, 1986) calculations. In this paper, we present the first step towards this goal, namely the sequential assignment of proton resonances using a combination of two-dimensional n.m.r. experiments, and the identification and delineation of secondary structure elements on the basis of a qualitative interpretation of the observed short-range NOEs. In addition, some long-range contacts are established and a low resolution tertiary structure proposed.

All n.m.r. experiments were carried out at 500 MHz on a Bruker AM500 spectrometer. The sample contained 6·8 mM-α1-purothionin (purified from Durum wheat as described by Mak & Jones, 1976*a*,*b*) in 500 mM-sodium phosphate buffer. Measurements were carried out at two pH values, pH 4·0 and 6·5, and at two temperatures, 25°C and 40°C. The following pure-phase absorption (Marion & Wüthrich, 1983) two-dimensional n.m.r. spectra were recorded in 90% H_2O/10% D_2O and 100% D_2O: DQF-COSY (Rance *et al.*, 1983), MLEV17 HOHAHA (Bax & Davis, 1985) and NOESY (Jeener *et al.*, 1979; Macura *et al.*, 1981). HOHAHA spectra (a variant of coherence transfer spectroscopy by isotropic mixing: Braunschweiler & Ernst, 1983) were recorded at several mixing times ranging from 15 to 80 milliseconds in order to demonstrate successively direct, single and multiple relayed through-bond magnetization transfer. NOESY spectra were recorded at mixing times of 100, 200 and 300 milliseconds. For measurements in H_2O, the H_2O resonance was suppressed by selective irradiation during the relaxation delay, and in the case of the NOESY spectra during the mixing time as well. An additional set of NOESY spectra in H_2O were also recorded without solvent irradiation by replacing the last 90° pulse in the sequence by a semi-selective jump–return pulse with the carrier placed at the position of the solvent (Plateau & Gueron, 1982).

Sequence-specific resonance assignments were obtained by first identifying amino acid spin systems by means of direct and relayed through-bond connectivities, followed by the sequential assignment of resonances by means of short (< 5 Å) through-space connectivities (Wüthrich *et al.*, 1982; Wagner & Wüthrich, 1982; Zuiderweg *et al.*, 1983; Clore *et al.*, 1986*b*; Zarbock *et al.*, 1986). The former were principally identified using the HOHAHA spectra, examples of which are shown in Figures 1 and 2 for the NH–aliphatic and CαH–aliphatic regions, respectively. The sequential assignment was carried out by identifying short-range NOEs involving the NH, CαH and CβH protons in the H_2O NOESY spectra. Some examples of these are shown in Figures 3 and 4 for the NH–NH and NH–aliphatic regions. With the exception of the first residue, Lys1, a continuous set of sequential

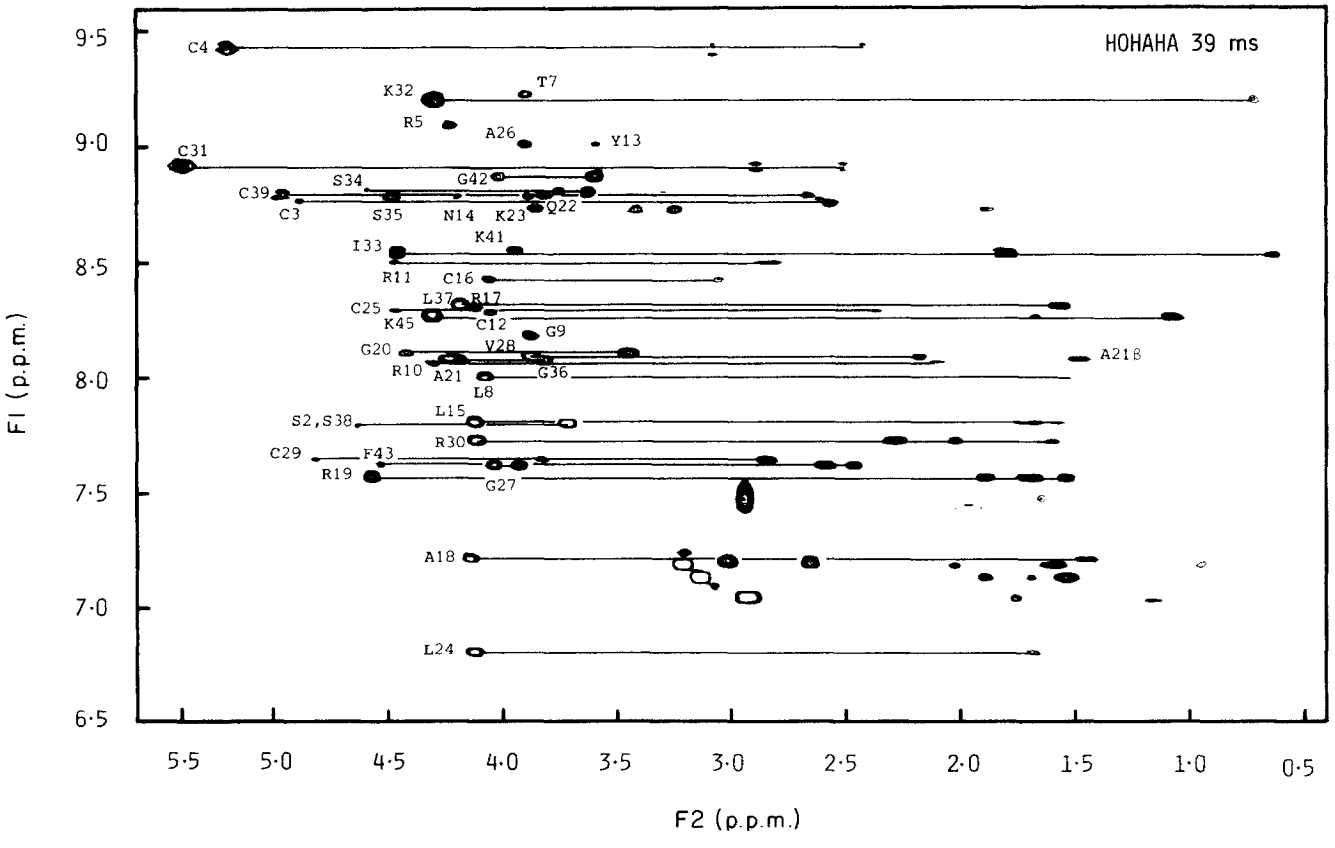

Figure 1. NH(F1 axis)–aliphatic(F2 axis) region of the HOHAHA spectrum of α1-purothionin in H_2O recorded at 25°C. Relayed connectivities are indicated by continuous lines and the labels are at the positions of the direct NH–CαH cross-peaks. The spectrum is unsymmetrized.

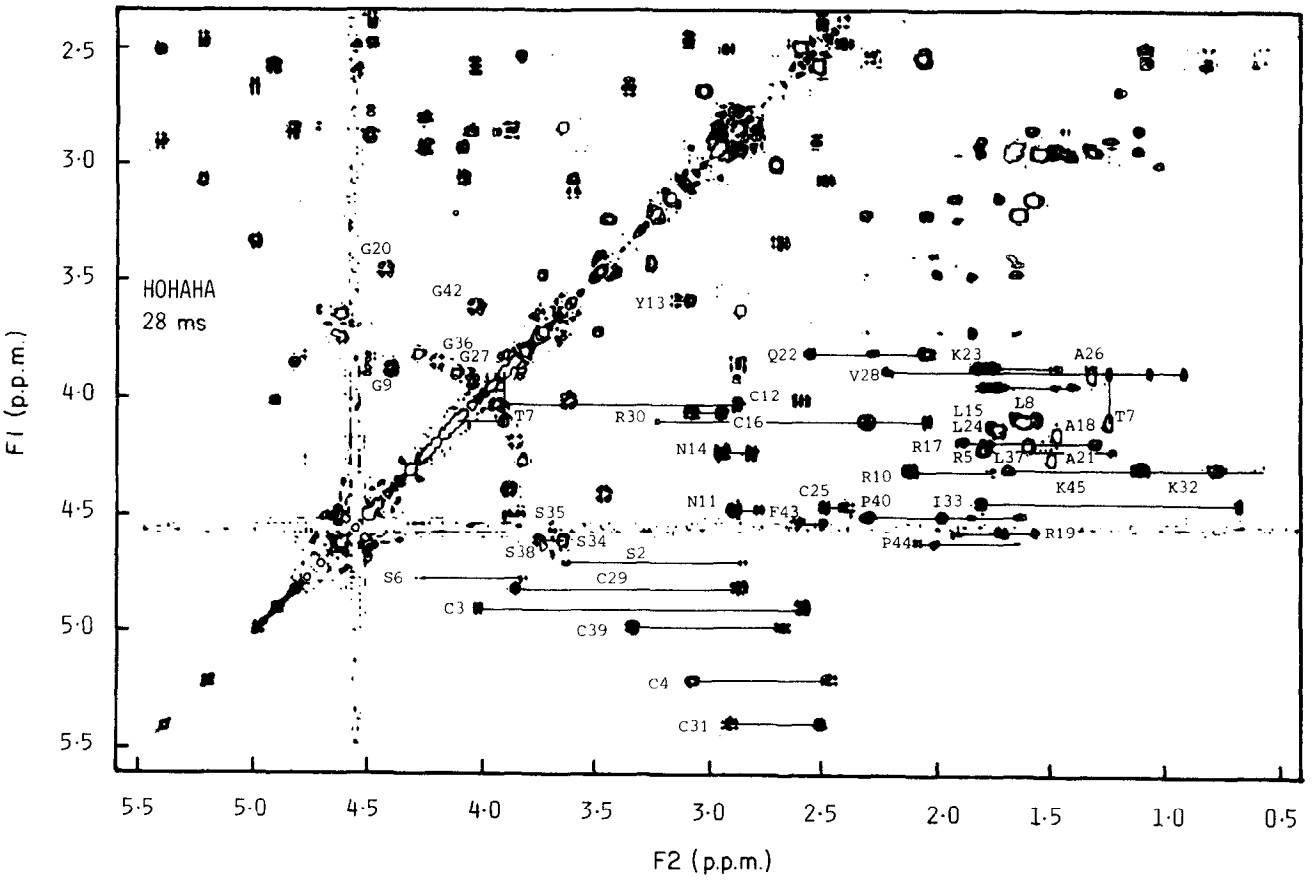

Figure 2. A portion of the CαH(F1 axis)–aliphatic(F2 axis) region of the HOHAHA spectrum of α1-purothionin in D_2O recorded at 40°C. Direct and relayed connectivities are present and spin systems originating from the CαH protons are indicated by continuous lines. The spectrum is symmetrized.

through-space connectivities along the polypeptide chain is observed. These are summarized in Figure 5 together with the $^3J_{HN\alpha}$ coupling constant data derived from the DQF-COSY spectrum and data on NH proton exchange. The assignments of the proton resonances at pH 4·0 and 25°C are given in Table 1.

The data in Figure 5 provide an easy means of identifying and delineating regular secondary structure elements (Wüthrich *et al.*, 1984; Pardi *et al.*, 1984; Kline & Wüthrich, 1985; Wagner *et al.*, 1986). Two helical segments are present, the first extending from residues 10 to 19 and the second from residues 23 to 28 (α1-purothionin numbering). These helices are characterized by a continuous stretch of strong $d_{NN}(i, i+1)$ NOEs, the presence of some medium strength $d_{\alpha N}(i, i+3)$ and/or $d_{\alpha\beta}(i, i+3)$ NOEs, weak or absent $d_{\alpha N}(i, i+1)$ NOEs, values of the apparent coupling constants $^3J_{HN\alpha} < 6$ Hz indicative of ϕ angles in the $-40°$ to $-90°$ range, and the presence of slowly exchanging NH protons. The observation of medium strength $d_{\alpha N}(i, i+1)$ NOEs between residues 25 and 26 and between residues 27 and 28 suggests the presence of some irregular features in the second helix. There are two short β-strands from residues 3 to 5 and 31 to 34, which are characterized by strong $d_{\alpha N}(i, i+1)$ NOEs, the absence of other short range NOEs (with the exception of $d_{\beta N}(i, i+1)$ NOEs which show little dependence on secondary structure), and values of the apparent $^3J_{HN\alpha}$ coupling constants >9 Hz indicative of ϕ angles in the $-80°$ to $-180°$ range. A mini antiparallel β-sheet is formed between these two strands and is manifested by the following long-range interstrand NOEs involving CαH and NH protons: a strong NOE between the CαH protons of Cys4 and Cys31, and medium-to-weak NOEs between the NH protons of Cys3 and Lys32, between the NH proton of Cys3 and the CαH proton of Ile33, between the CαH proton of Cys4 and the NH proton of Lys32, and between the NH proton of Arg5 and the CαH proton of Cys31. This is further supported by the observation that the NH protons of Cys3 and Lys32 exchange slowly, consistent with them hydrogen bonding to the carbonyl oxygen atom of Lys32 and Cys3, respectively. Further, the two strands are held together by a disulphide bond between Cys4 and Cys31.

In addition to helices and β-strands, a number of turns can also be identified by inspection of the short-range NOEs (Wagner *et al.*, 1986). These comprise residues 6 to 9, 20 to 22, 29 to 30, 35 to 38 and 40 to 43. The segment from residues 35 to 38 can further be classified as a half-turn (Wagner *et al.*, 1986) characterized by strong $d_{\alpha N}(i, i+1)$ and

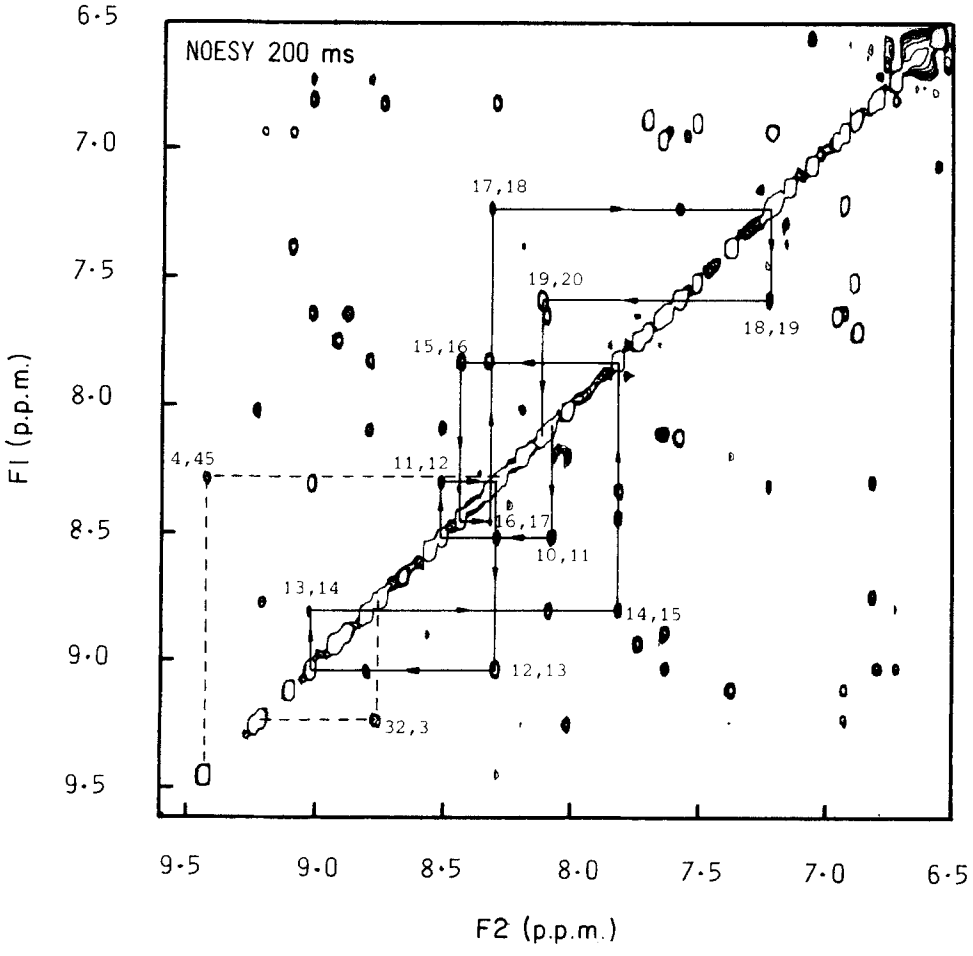

Figure 3. NH(F1 axis)–NH(F2 axis) region of the 200 ms NOESY spectrum of α1-purothionin in H_2O recorded at 25°C. The sequence of $d_{NN}(i, i+1)$ connectivities extending from Arg10 to Gly20 comprising helix A (residues 10 to 19) is indicated by continuous lines. Two long-range connectivities are indicated by broken lines. The spectrum was recorded using the jump–return sequence for the last 90° pulse to suppress the water resonance. The spectrum is unsymmetrized.

absent $d_{NN}(i, i+1)$ NOEs between residues 36 and 37, strong $d_{NN}(i, i+1)$ and absent $d_{\alpha N}(i, i+1)$ NOEs between residues 37 and 38, and values of $^3J_{HN\alpha} < 8$ Hz for Leu37 ($\phi \sim -60°$) and >8 Hz for Ser38 ($\phi \sim -90°$).

Table 2 shows the comparison of the secondary structure of α1-purothionin as determined by n.m.r. with that of the X-ray structure of crambin (Hendrickson & Teeter, 1981). Crambin is one residue longer than α1-purothionin and the highest degree of sequence homology is obtained by deleting residue 24 of crambin (Teeter *et al.*, 1981). The secondary structures of the two proteins are clearly similar although some differences are apparent. It should be borne in mind, however, that the comparison is between a crystal structure (i.e. crambin) and a solution structure (i.e. α1-purothionin), so that some of the differences that are observed may simply reflect differences in local mobility and/or disorder between the crystal and solution structures. For example, β-strand 1 starts earlier and is longer in crambin than in α1-purothionin. This is in part because the first two residues of α1-purothionin do not display the features of a regular β-strand (i.e. very strong $d_{\alpha N}(i, i+1)$ NOEs). Moreover, Ser2 of α1-purothionin is not part of the β-sheet formed by strands 1 and 2 as no NOE between the CαH protons of Ser2 and Ile33 could be detected. Helix A is longer in crambin (residues 7 to 19) than in α1-purothionin (residues 10 to 19). This finding is in accord with laser Raman studies on crambin and α1-purothionin in solution which suggested that residues 5 to 11 in both proteins formed either a 3–10 helix or a turn (Williams & Teeter, 1984). c.d. analysis and secondary structure prediction of α1-purothionin suggested a turn at residues 10–11 (M. Whitlow & M. M. Teeter, unpublished results). In fact, residues 6 to 9 constitute a turn in α1-purothionin. The turn between the two helices is in the same position in the two proteins. Helix B is two residues shorter in α1-purothionin than in crambin, but as in crambin it appears to be less regular than helix A. Helix B leads to a turn in both α1-purothionin (residues 29 to 30) and crambin (residue 31, which is equivalent to residue 30 in α1-purothionin). This is followed by strand 2 which occupies equivalent positions in the two proteins, as do (approximately) the remaining two turns.

A comparison of the secondary structure

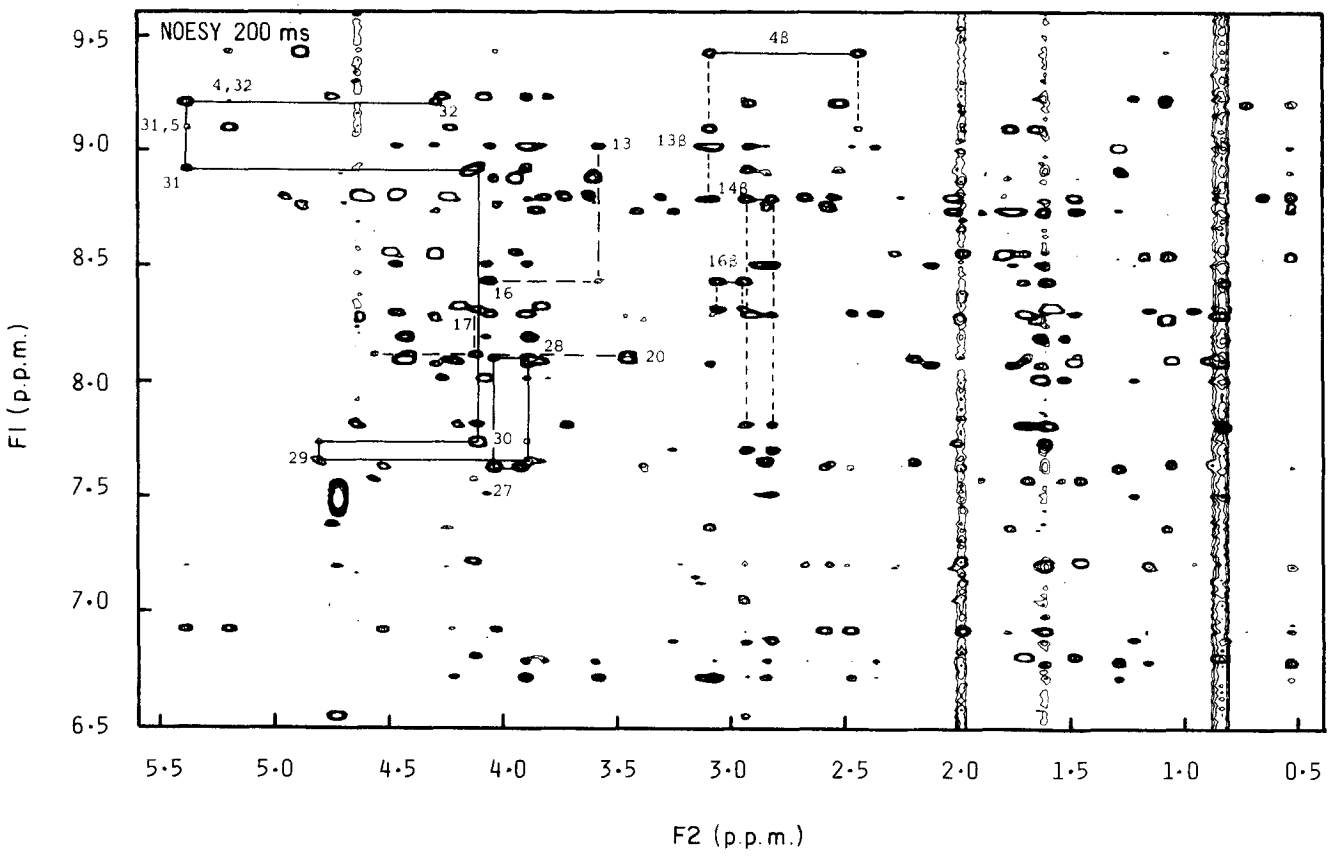

Figure 4. NH(F1 axis)–aliphatic(F2 axis) region of the 200 ms NOESY spectrum of α1-purothionin in H_2O recorded at 25°C. Some $d_{\alpha N}(i, i+1)$ and $d_{\alpha N}(i, i+3)$ connectivities are indicated by the symbols —— and – – –, respectively. Peaks are labelled at the position of the NH(i)–CαH(i) intraresidue cross-peaks. Also indicated are some $d_{\beta N}(i, i+1)$ connectivities (– – – – –). The spectrum was recorded using the jump–return sequence for the last 90° pulse to suppress the water resonance. The spectrum is unsymmetrized.

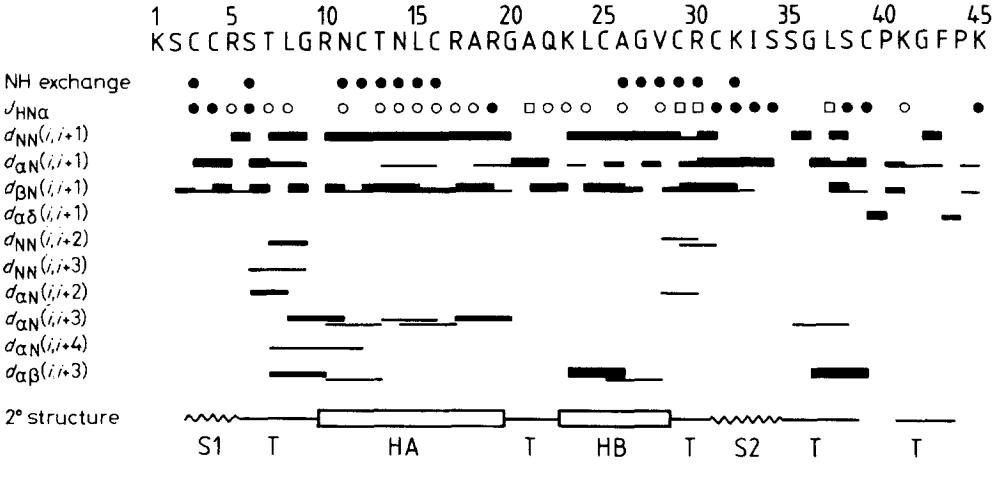

Figure 5. The sequence of α1-purothionin together with a summary of the observed short-range interresidue NOEs involving the NH, CαH and CβH protons. The NOEs are classified into strong, medium and weak by the thickness of the line. NH protons that are still present after dissolving the protein in D_2O are indicated by filled circles. (Note that all NH protons exchange virtually completely after 3 h at 25°C and at pH 4.) Apparent values of $^3J_{HN\alpha} < 6$ Hz, 6 Hz $< {}^3J_{HN\alpha} < 9$ Hz and $^3J_{HN\alpha} > 9$ Hz, as measured from the DQF-COSY spectrum, are indicated by the symbols ○, □ and ●, respectively.

Table 1

Proton resonance assignments of α1-purothionin at 25°C and pH 4

Residue	Chemical shift (p.p.m.) NH	CαH	CβH	Others
Lys1		4·15		CγH 1·69, 1·67; CδH 1·16, 0·97; CεH 3·04, 2·69; NζH 7·20
Ser2	7·82	4·66	3·73, 2·84	
Cys3	8·76	4·90	4·03, 2·58	
Cys4	9·43	5·21	3·09, 2·44	
Arg5	9·10	4·24	1·79, 1·67	CγH 1·24; CδH 2·91; NεH 7·04
Ser6	7·38	4·77	4·29, 3·84	
Thr7	9·23	3·90	4·09	CγH 1·23
Leu8	8·01	4·09	1·63, 1·54	CγH 1·58; CδH 0·90, 0·85
Gly9	8·20	4·44, 3·89		
Arg10	8·08	4·31	2·11, 2·11	CγH 1·91, 1·76; CδH 3·42, 3·27; NεH 8·73
Asn11	8·51	4·48	2·89, 2·81	NH_2 7·52, 6·88
Cys12	8·29	4·07	3·91, 2·85	
Tyr13	9·02	3·58	3·12, 3·07	CδH 6·72; CεH 6·80
Asn14	8·80	4·22	2·93, 2·83	NH_2 7·72, 6·87
Leu15	7·82	4·13	1·70, 1·64	CγH 1·48; CδH 0·89, 0·86
Cys16	8·43	4·07	3·06, 2·94	
Arg17	8·31	4·13	1·90, 1·78	CγH1·55, 1·31; CδH 2·97; NεH 7·04
Ala18	7·22	4·14	1·46	
Arg19	7·58	4·58	1·90, 1·71	CγH 1·56, 1·56; CδH 3·15; NεH 7·14
Gly20	8·12	4·43, 3·46		
Ala21	8·10	4·25	1·58	
Gln22	8·80	3·82	2·03, 2·03	CγH 2·55, 2·25; NH_2 7·65, 6·95
Lys23	8·74	3·87	1·82, 1·76	CγH 1·48, 1·34; CδH 1·65; CεH 2·89; NζH 7·48
Leu24	6·82	4·13	1·71, 1·71	CγH 1·71; CδH 0·85, 0·85
Cys25	8·30	4·48	2·47, 2·37	
Ala26	9·02	3·91	1·29	
Gly27	7·63	4·05, 3·93		
Val28	8·11	3·89	2·18	CγH 1·05, 0·90
Cys29	7·66	4·82	3·83, 2·84	
Arg30	7·73	4·12	2·30, 2·00	CγH 1·61, 1·61; CδH 3·22; NεH 7·20
Cys31	8·92	5·40	2·92, 2·52	
Lys32	9·21	4·31	1·12, 0·79	CγH 0·61, 0·58; CδH 1·09, 0·85; CεH 2·59, 2·52
Ile33	8·56	4·46	1·79	CγH 1·20, 1·05; $Cγ_MH$ 0·68; CδH 0·58
Ser34	8·80	4·61	3·74, 3·63	
Ser35	8·81	4·48	3·90, 3·83	
Gly36	8·08	4·19, 3·83		
Leu37	8·32	4·20	1·58, 1·58	CγH 1·58; CδH 0·86, 0·80
Ser38	7·81	4·65	3·75, 3·75	
Cys39	8·80	4·97	3·31, 2·67	
Pro40		4·50	2·31, 1·99	CγH 1·86, 1·65; CδH 3·74, 3·50
Lys41	8·56	3·95	1·80, 1·75	CγH 1·50, 1·42; CδH 1·69; CεH 2·96; NζH 7·48
Gly42	8·88	4·03, 3·61		
Phe43	7·64	4·53	2·60, 2·58	CδH 6·93; CεH 7·21; CζH 7·21
Pro44		4·64	2·10, 2·03	CγH 1·66, 1·66; CδH 3·48, 3·40
Lys45	8·28	4·31	1·70, 1·12	CγH 1·12; CδH 1·56, 1·42; CεH 2·95, 2·85; NζH 7·48

p.p.m., parts per million.

fractions from our results with those derived from c.d. and laser Raman spectroscopy is of interest (Table 3). This shows that both the c.d. and Raman analyses resulted in larger fractions of β-sheet and a smaller fraction of turns (M. M. Teeter & M. Whitlow, unpublished results; Williams & Teeter, 1984) than the n.m.r. data indicate is present. It should be noted, however, that both the c.d. and Raman analyses correctly predicted the two helices and most of the turns.

At present time we are still in the process of assigning all the long-range NOE cross-peaks. Nevertheless, a number of these have been clearly identified and are summarized in Figure 6. The low resolution spatial structure of α1-purothionin can be modelled on the basis of these NOEs by simply considering the secondary structure elements as rigid bodies. The long axes of the two helices are approximately parallel to each other. This relative orientation is determined not only by the two disulphide bonds between Cys12 and Cys29 and between Cys16 and Cys25 but also by numerous interhelix NOEs, in particular between Cys12 and Ala26, Tyr13 and Cys25, Tyr13 and Ala26, Cys16 and Val28, and Ala18 and Cys29. The angle between the long axes of the helices and the long axis of the β-sheet lies in the range 30° to 60° and is determined by the NOEs between residues of strand

Table 2

Comparison of the secondary structure of α1-purothionin in solution as determined by n.m.r. with that of crambin as determined by X-ray crystallography

	α1-Purothionin	Crambin†
Helix A	10–19	7–19
Helix B	23–28	23–30
β-Strand 1	3–5	1–4
β-Strand 2	31–34	32–35
Turns	6–9	5–6
	20–22	20–22
	29–30	31
	35–38	36–38
	41–43	41–44

† From Hendrickson & Teeter (1981). Crambin is one residue longer than α1-purothionin and the highest degree of homology is found by deleting residue 24 (Teeter *et al.*, 1981).

Table 3

Comparison of the secondary structure fractions of α1-purothionin determined by n.m.r. with those predicted by c.d. and laser Raman spectroscopy

	Fraction			
Technique	Helix	Sheet	Turn	Random
n.m.r.	0·36	0·16	0·36	0·13
c.d.†	0·33	0·32	0·16	0·19
Raman‡	0·36	0·28	0·19	0·16

† From Whitlow & Teeter (unpublished results).
‡ From Williams & Teeter (1984) where the results were unconstrained (*R*2).

1 and helix A (*viz* between Lys1 and Tyr13, Ser2 and Tyr13, and Cys4 and Arg10), and between Ile33 of strand 2 and Tyr13 and Lys23 of helices A and B, respectively. Strand 2 leads into a half-turn (residues 35 to 38), which carries the chain round the end of strand 1 and back along strand 1 such that the remaining residues (39 to 45) are in close proximity to strand 1. This is manifested by the NOEs between Cys3 and Cys39, from Cys3, Cys4 and Arg5 to Phe43, between Arg5 and Pro44, and from Cys4, Ser6 and Thr7 to Lys45. The orientation of residues 39 to 45 relative to strand 1 is also constrained by the disulphide bond between Cys3 and Cys39. Additionally, the aromatic ring of Phe43 is close to the side-chain of Lys32. Thus, the overall structure has the shape of a Γ with the arm comprising the helices being longer than that comprising the antiparallel β-sheet and residues 35 to 45.

Both the secondary structural features as well as the low resolution tertiary structure derived from the NOE data are clearly similar to those of crambin (Hendrickson & Teeter, 1981). We are now in the process of determining a high resolution structure of α1-purothionin by means of restrained molecular dynamics (Brünger *et al.*, 1986; Clore *et al.*, 1986*a*) on the basis of distance and dihedral angle restraints derived from the NOE and coupling constant data. Once this is complete, a detailed comparison of the two structures as well as a comparison with the proposed model of α1-purothionin (Whitlow & Teeter, 1985) will be possible.

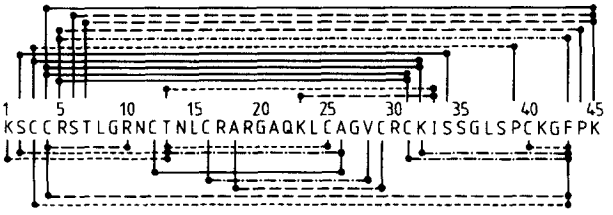

Figure 6. Summary of the long-range NOEs assigned at the present time. The symbols used are as follows: (———) backbone–backbone NOEs; (– – –) backbone–side-chain NOEs; (– – – – –) side-chain–side-chain NOEs; (– · – · –) backbone–side-chain plus side-chain–side-chain NOEs; and (– · – · – · –) backbone–backbone plus backbone–side-chain plus side-chain–side-chain NOEs.

This work was supported by the Max-Planck Gesellschaft (G.M.C. and A.M.G.). We thank Professor Martin Karplus for useful discussions.

G. Marius Clore
Dinesh K. Sukumaran
Angela M. Gronenborn

Max-Planck-Institut für Biochemie
D-8033 Martinsried bei München, FRG

Martha M. Teeter
Marc Whitlow

Department of Chemistry and Biochemistry
Boston University
685 Commonwealth Avenue
Boston, MA 02215, U.S.A.

Berne L. Jones

Cereal Crops Research Unit
United States Department of Agriculture, ARS
501 N. Walnut Street
Madison, WI 53705, U.S.A.

Received 25 June 1986, and in revised form
1 October 1986

References

Anderson, K. & Johannson, M. (1973). *Eur. J. Biochem.* **32**, 223–231.

Bax, A. & Davis, D. G. (1985). *J. Magn. Reson.* **65**, 355–360.

Braun, W. & Go, N. (1985). *J. Mol. Biol.* **186**, 611–626.

Braunschweiler, L. & Ernst, R. R. (1983). *J. Magn. Reson.* **53**, 521–528.

Brünger, A. T., Clore, G. M., Gronenborn, A. M. & Karplus, M. (1986). *Proc. Nat. Acad. Sci., U.S.A.* **83**, 3801–3805.

Carrasco, L., Vazquez, D., Hernandez-Lucus, C., Carbonero, P. & Garcia-Olmedo, F. (1971). *Eur. J. Biochem.* **116**, 185–189.

Clore, G. M., Gronenborn, A. M., Brünger, A. T. & Karplus, M. (1985). *J. Mol. Biol.* **186**, 435–455.
Clore, G. M., Brünger, A. T., Karplus, M. & Gronenborn, A. M. (1986*a*). *J. Mol. Biol.* **191**, 523–551.
Clore, G. M., Martin, S. R. & Gronenborn, A. M. (1986*b*). *J. Mol. Biol.* **191**, 553–561.
Havel, T. F. & Wüthrich, K. (1985). *J. Mol. Biol.* **182**, 281–294.
Hendrickson, W. A. & Teeter, M. M. (1981). *Nature (London)*, **290**, 107–113.
Jeener, J., Meier, B. H., Bachmann, P. & Ernst, R. R. (1979). *J. Chem. Phys.* **71**, 4546–4553.
Jones, B. L., Lockhart, G. L., Mak, A. & Cooper, D. B. (1982). *J. Hered.* **73**, 143–144.
Kaptein, R., Zuiderweg, E. R. P., Scheek, R. M., Boelens, R. & van Gunsteren, W. F. (1985). *J. Mol. Biol.* **182**, 179–182.
Kline, A. D. & Wüthrich, K. (1985). *J. Mol. Biol.* **183**, 503–507.
Kline, A. D., Braun, W. & Wüthrich, K. (1986). *J. Mol. Biol.* **189**, 377–382.
Lecomte. J. T. J., Jones, B. L. & Llinas, M. (1982). *Biochemistry*, **21**, 4843–4849.
Macura, S., Huang, Y., Suter, D. & Ernst, R. R. (1981). *J. Magn. Reson.* **43**, 259–281.
Mak, A. S. & Jones, B. L. (1976*a*). *Canad. J. Biochem.* **54**, 835–842.
Mak, A. S. & Jones, B. L. (1976*b*). *J. Sci. Food Agric.* **27**, 205–213.
Marion, D. & Wüthrich, K. (1983). *Biochem. Biophys. Res. Commun.* **113**, 967–974.
Okada, T. & Vashizumi, H. (1973). *Agric. Biol. Chem.* **37**, 2289–2294.
Pardi, A., Billeter, M. & Wüthrich, K. (1984). *J. Mol. Biol.* **180**, 741–751.
Plateau, P. & Gueron, M. (1982). *J. Amer. Chem. Soc.* **104**, 7310–7311.
Rance, M., Sorenson, O. W., Bodenhausen, G., Wagner, G., Ernst, R. R. & Wüthrich, K. (1983). *Biochem. Biophys. Res. Commun.* **117**, 479–485.
Teeter, M. M. & Hendrickson, W. A. (1979). *J. Mol. Biol.* **127**, 219–223.
Teeter, M. M. & Kossiakoff, A. A. (1982). In *Neutrons in Biology* (Schoenborn, V., ed.), pp. 335–348, Plenum Press, New York.
Teeter, M. M., Mazer, J. A. & L'Italien, J. J. (1981). *Biochemistry*, **20**, 5437–5443.
Van Etten, C. H., Nielsen, H. C. & Peters, J. E. (1965). *Phytochemistry*, **4**, 219–223.
Wada, K. & Buchanan, B. B. (1981). *FEBS Letters*, **124**, 237–240.
Wagner, G. & Wüthrich, K. (1982). *J. Mol. Biol.* **160**, 343–361.
Wagner, G., Neuhaus, D., Wörgötter, E., Vasak, M., Kägi, J. H. R. & Wüthrich, K. (1986). *J. Mol. Biol.* **187**, 131–135.
Whitlow, M. (1986). Ph.D thesis, Boston University, Boston, MA.
Whitlow, M. & Teeter, M. M. (1985). *J. Biomol. Struct. Dynam.* **2**, 831–848.
Williams, R. W. & Teeter, M. M. (1984). *Biochemistry*, **23**, 6796–6802.
Williamson, M. P., Havel, T. F. & Wüthrich, K. (1985). *J. Mol. Biol.* **182**, 295–315.
Wüthrich, K., Wider, G., Wagner, G. & Braun, W. (1982). *J. Mol. Biol.* **155**, 311–319.
Wüthrich, K., Billeter, M. & Braun, W. (1984). *J. Mol. Biol.* **180**, 715–740.
Zarbock, J., Clore, G. M. & Gronenborn, A. M. (1986). *Proc. Nat. Acad. Sci., U.S.A.* **83**, 7628–7632.
Zuiderweg, E. R. P., Kaptein, R. & Wüthrich, K. (1983). *Eur. J. Biochem.* **127**, 279–292.

Edited by M. F. Moody